An Easily Synthesized Blue Polymer for High-Performance Polymer Solar Cells

By *Ergang Wang,* Lintao Hou, Zhongqiang Wang, Stefan Hellström, Fengling Zhang, Olle Inganäs,* and *Mats R. Andersson**

Dedicated to Prof. Yong Cao on the occasion of his 70th birthday.

The need for renewable energy supply is driving new technologies for photovoltaic energy conversion. Polymer solar cells are a promising sustainable solar energy converter, because of the unique advantages of low cost, light weight, and potential use in flexible devices.[1–3] So far, the most efficient polymer solar cell system is built on the concept of bulk heterojunction (BHJ) structure, which uses a blend of an electron-rich polymer as donor and an electron-poor fullerene as acceptor.[4,5] In this case, the BHJ structure not only provides a large-area donor-acceptor interface for charge separation but also may form a bicontinuous interpenetrating network for charge transport. Based on the BHJ structure, polymer solar cells made by a blend of poly(3-hexylthiophene) (P3HT) and [6,6]-phenyl-C_{61}-butyric acid methyl ester ([60]PCBM) were intensively investigated with power conversion efficiencies (PCE) up to 5%.[6,7] Yet, the PCE of P3HT-based solar cells was mainly limited by low open circuit-voltage (V_{oc}) and its narrow absorption spectrum ranging from 300 to 650 nm, with major loss of the solar radiation. Recently, low bandgap polymers with broad absorption spectra were developed, with PCEs over 6% using [6,6]-phenyl-C_{71}-butyric acid methyl ester ([70]PCBM) as acceptor.[8,9] This achievement enhanced the confidence in the commercialization of polymer solar cells.

A facile method to synthesize low bandgap polymers was developed, which combined electron-rich unit (donor) and electron deficient unit (acceptor) in their repeating units forming internal donor-acceptor (D-A) structures. By using this method, a series of low bandgap polymers based on polyfluorenes were investigated, which showed efficiencies of 2–4.5%.[10–14] Very recently, a poly(2,7-carbazole) derivative showed PCE over 6%.[9] Several other D-A type polymers also showed PCEs of 5–6%.[8,15–18] However, the synthesis of these low bandgap polymers is complicated with relatively long synthetic routes and low yields. For application in large-area polymer solar cells, it is critical to obtain easily synthesized polymers with low cost. Here, we report an easily synthesized D-A type of low bandgap polymer based on thiophene and quinoxaline named poly[2,3-bis-(3-octyloxyphenyl)quinoxaline-5,8-diyl-*alt*-thiophene-2,5-diyl] (TQ1) (**Scheme 1**) and its application in polymer solar cells. This polymer structure and its optical properties have previously been disclosed by Yamamoto et al.[19] Recently, several similar polymers with different side chains were synthesized with low molecular weights, showing poor photovoltaic performance.[20,21] Yet, considering the promising photophysical properties of TQ1, it should be interesting to investigate its photovoltaic performance. In this paper, we modify the synthesis of TQ1 and investigate its optical, electrochemical and photovoltaic properties. After early optimization of the preparation of the solar cells, a maximum power point (MPP) up to 6 mW m^{-2} was achieved with a high V_{oc} of ca. 0.9 V from a blend of TQ1 and [70]PCBM under illumination from an air mass 1.5 global (AM 1.5G) solar simulator (100 mW cm^{-2}).

The monomers 2,5-bis(trimethylstannyl)thiophene (**2**) and 4,7-dibromobenzo[c][1,2,5]thiadiazole are commercially available. The synthesis of the monomer 5,8-dibromo-2,3-bis(3-(octyloxy)phenyl)quinoxaline (**1**) was modified and a much higher overall yield of 61.6% (include the yield 70% of 1,2-bis(3-(octyloxy)phenyl)ethane-1,2-dione synthesized by following the literature.[22]) was obtained compared to the previously reported yield of 20–30%.[19] The monomer **1** was synthesized by condensation of the reduction product of 4,7-dibromobenzo[c][1,2,5]thiadiazole with 1,2-bis(3-(octyloxy)phenyl)ethane-1,2-dione via two successive steps in high yield. Therefore, TQ1 can be easily synthesized by polymerization of the monomers **1** and **2** via modified Stille coupling with a rather short synthetic route, compared to other low bandgap polymers mentioned above. To remove the catalyst and avoid the influence of metal in the performance of the resulting solar cells, the polymer was purified by washing with sodium diethyldithiocarbamate trihydrate solution and Soxhlet extraction with diethyl ether and chloroform.[23] After purification, the molecular weight was investigated by size exclusion chromatography (SEC) relative to monodisperse polystyrene standards, which showed a relatively high number average molecular weight (M_n) of 41,000 with a polydispersity index (*PDI*) of 2.6. Octyloxy was chosen as the side chain of quinoxaline to ensure good solubility of the resulting polymer in organic solvents and suitable miscibility with the fulleride acceptor. As a result, the polymer is readily soluble in common solvents such as tetrahydrofuran,

[*] Dr. E. Wang, S. Hellström, Dr. F. Zhang, Prof. M. R. Andersson
Department of Chemical and Biological
Engineering/Polymer Technology
Chalmers University of Technology
SE-412 96 Göteborg (Sweden)
E-mail: ergang@chalmers.se; mats.andersson@chalmers.se
Dr. L. Hou, Z. Wang, Prof. O. Inganäs
Biomolecular and Organic Electronics
IFM, and Center of Organic Electronics
Linköping University
SE-581 83 Linköping (Sweden)

DOI: 10.1002/adma.201002225

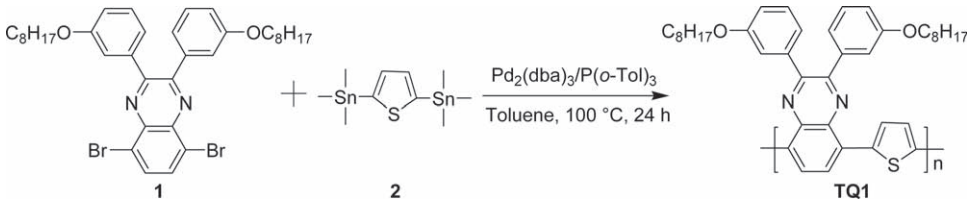

Scheme 1. Synthesis of the polymer TQ1.

chloroform, chlorobenzene and *o*-dichlorobenzene (ODCB). Unlike many low bandgap polymers that appear red, purple, black or green in color, the deep blue color of the polymer both in solution and in film is quite attractive (see **Figure 1**). The polymer exhibited a reasonable thermal stability with a degradation temperature of 300 °C (5% weight loss) as tested by thermal gravimetric analysis (TGA).

As shown in Figure 1, the absorption spectra of TQ1 both in film and in ODCB solution at 20 °C present two absorption bands. The absorption bands in film peak at 360 nm and 620 nm, and are broader than that in solution, where peaks are found at 358 nm and 612 nm. It is worth noting that the λ_{max} position of TQ1 in film has no obvious red-shift compared with that in solution at 20 °C. For the absorption spectra of many conjugated polymers, there is a red-shift that occurs in going from the solution to the solid state because of the aggregation of the polymer chains in the solid state.[24,25] Judged from the planar and rigid polymer chain, the reason for the absent red-shift may originate from the aggregation of the polymer chains formed in solution. To verify our supposition, the absorption spectrum of the polymer was measured in ODCB solution at 100 °C. As shown in Figure 1, the absorption spectrum of the polymer in ODCB solution at 100 °C has a λ_{max} at 333 nm and 555 nm, showing an obvious blue shift of 57 nm compared to the one measured at 20 °C. The blue shift can be attributed to breakup of interchain aggregates in solution.[25,26] In this case, the polymer is molecularly dissolved in ODCB at 100 °C, which is consistent with our supposition. Meanwhile, the broader absorption spectrum in the solid state indicates an orderly π–π stacking formed in the solid state, which is related to its semi-crystalline structure disclosed previously.[19] The optical bandgap deduced from the onset (730 nm) of the polymer absorption spectrum in film is 1.70 eV, which is promising for solar cell applications.

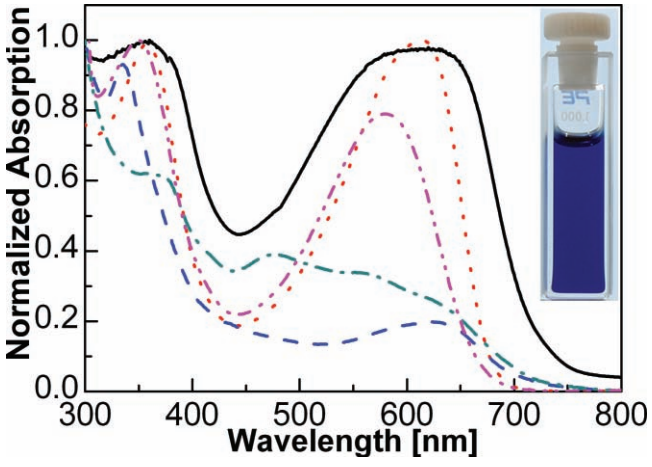

Figure 1. UV-vis spectra of TQ1 in film (solid line), in ODCB solution measured at 20 °C (dotted line) and at 100 °C (dash dot dotted line); UV-vis spectra from the films of the blend of TQ1:[60]PCBM = 1:3 (dashed line) and TQ1:[70]PCBM = 1:3 (dash dotted line). The insert is the image of TQ1 in chloroform solution.

To estimate the band positions of the polymer, the highest occupied molecular orbital (HOMO) and lowest unoccupied molecular orbital (LUMO) levels of the polymer were investigated by square-wave voltammetry (SWV).[27] The HOMO and LUMO levels, calculated from oxidation and reduction peak potentials, are −5.7 eV and −3.3 eV, respectively. The high LUMO level of TQ1 ensures a downhill driving force for charge separation to [60]PCBM or [70]PCBM, whose LUMO levels have been previously reported to be −4.1 eV measured under the same experimental conditions.[27] Considering the low HOMO level of TQ1, a high V_{oc} can be expected.[28] The study of photophysical and electrochemical properties of TQ1 indicates this polymer is a highly promising candidate for polymer solar cells.

The polymer solar cells were fabricated from a blend of TQ1:[60]PCBM (the optimized weight ratio is 1:3) in chloroform solution. In this condition, a MPP of 3.0 mW cm^{-2} with a V_{oc} of 0.90 V, a short-circuit current density (J_{sc}) of 5.9 mA cm^{-2} and a fill factor (*FF*) of 0.56 was obtained under illumination from an AM 1.5G solar simulator (100 mW cm^{-2}). The high V_{oc} of the devices demonstrates the advantage of the low HOMO level of TQ1. The morphology of the active layer is very important for polymer solar cells, and can influence charge separation and transport. To gain insight into the morphology of the active layer, atomic force microscopy (AFM) was used to investigate the surface of the film from a blend of TQ1:[60]PCBM = 1:3 in chloroform solution. As shown in **Figure 2a**, large domains (about 200–400 nm in diameter) on the surface of the film with root mean square (RMS) of 2.57 nm indicate non-optimal morphology, which is not favorable for charge separation and transport and thus limits the efficiency of the resulting devices. To modify the morphology of the film, ODCB was used as the solvent to dissolve the blend of TQ1:[60]PCBM = 1:3. The devices fabricated under this condition show a MPP of 4.9 mW cm^{-2} with a V_{oc} of 0.86 V, a J_{sc} of 9.4 mA cm^{-2} and a *FF* of 0.60. The reason for the dramatic enhancement of photovoltaic performance can be found in the AFM image (Figure 2b) of the film spin-coated from the ODCB solution of TQ1:[60]PCBM = 1:3, which shows much smaller domains with RMS of 1.09 nm. The smoother urface indicates good miscibility between TQ1 and [60]PCBM without large phase separation, resulting in the increase of J_{sc} and *FF*.

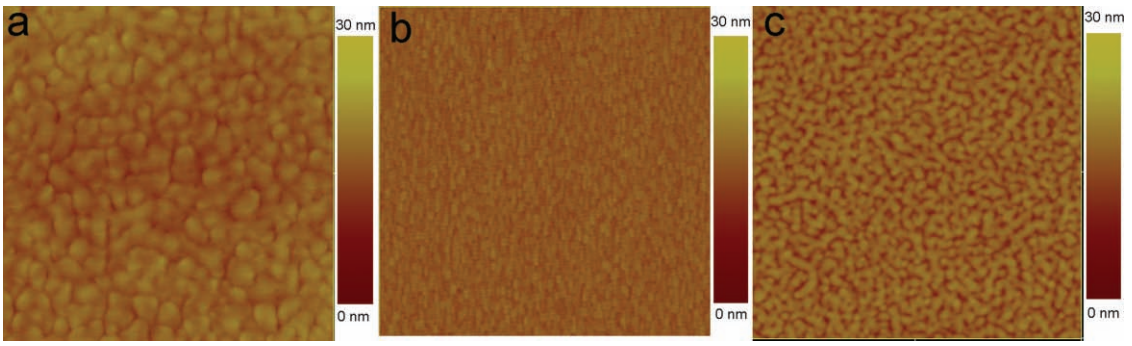

Figure 2. Topography of AFM images (5 μm × 5 μm). a) TQ1:[60]PCBM = 1:3 from chloroform. b) TQ1:[60]PCBM = 1:3 from ODCB. c) TQ1:[70]PCBM = 1:3 from ODCB.

[70]PCBM has similar electronic properties to [60]PCBM, but a considerable higher absorption-coefficient in visible region because of its asymmetric chemical structure.[29] To compensate the valley of the absorption spectrum of TQ1 around 450 nm, [70]PCBM was used as the acceptor instead of [60]PCBM to improve the performance of the resulting solar cells.[30] As shown in Figure 1, the absorption intensity from a blend of TQ1:[70]PCBM = 1:3 has obvious improvement in the visible region compared with that of TQ1:[60]PCBM = 1:3. Therefore, a higher MPP can be expected from the devices of TQ1:[70]PCBM. The ratio of TQ1:[70]PCBM were optimized from 1:2, 1:3 to 1:4. All the parameters for the three kinds of typical high performing solar cells are summarized in **Table 1** and present comparable performance with J_{sc} of 9–10 mA cm^{-2}, V_{oc} about 0.89 V, *FF* above 0.6 and MPP from 5.7 mW cm^{-2} to 6.0 mW cm^{-2}. It is striking that the performance of the solar cells are not sensitive to the ratio of two components, which simplifies the preparation of devices, since it's not necessary to control the ratio of TQ1:[70]PCBM strictly. With a ratio of TQ1:[70]PCBM = 1:3, a MPP of 6.0 mW cm^{-2} with a V_{oc} of 0.89 V, a J_{sc} of 10.5 mA cm^{-2} and a fill factor (*FF*) of 0.64 was achieved under illumination from an AM 1.5G solar simulator (100 mW cm^{-2}). It was noted that this performance was achieved by simply fabricated devices without annealing, additive or extra layers, which is beneficial for preparation of low cost polymer solar cells. To understand the high performance of this device, the surface of the film made from the ODCB solution of TQ1:[70]PCBM = 1:3 was also investigated by AFM, which showed fairly fine features with RMS of 3.2 nm (Figure 2c). For comparison, the *J*–*V* curves from the solar cells of TQ1:[60]PCBM = 1:3 fabricated from chloroform solution, ODCB solution and the one from TQ1:[70]PCBM = 1:3 are plotted together in **Figure 3**. All of them show quite high *FF* and almost identical V_{oc}. To confirm the accuracy

Table 1. Photovoltaic parameters of the devices.

Weight ratio	Solvent	J_{sc} [mA cm^{-2}]	V_{oc} [V]	*FF*	MPP [mW cm^{-2}]
TQ1:[60]PCBM = 1:3	Chloroform	5.9	0.90	0.56	3.0
TQ1:[60]PCBM = 1:3	ODCB	9.4	0.86	0.60	4.9
TQ1:[70]PCBM = 1:2	ODCB	9.4	0.91	0.68	5.8
TQ1:[70]PCBM = 1:3	ODCB	10.5	0.89	0.64	6.0
TQ1:[70]PCBM = 1:4	ODCB	10.1	0.89	0.63	5.7

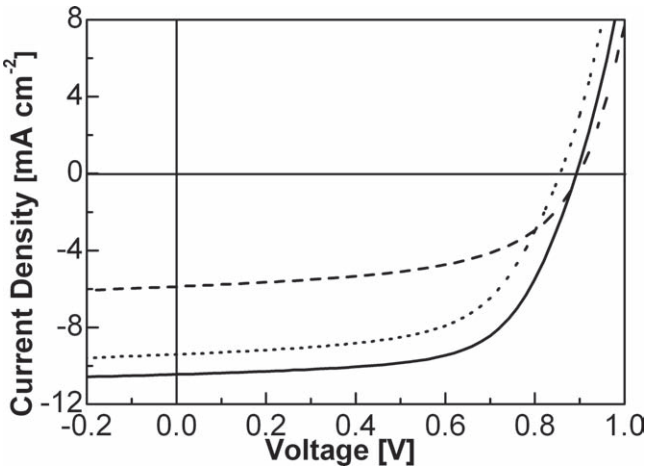

Figure 3. *J*–*V* curves of the devices from TQ1:[60]PCBM = 1:3 in chloroform solution (dashed line), TQ1:[60]PCBM = 1:3 in ODCB solution (dotted line) and TQ1:[70]PCBM = 1:3 in ODCB solution (solid line).

of the measurement of the devices, their corresponding external quantum efficiency (EQE) were measured under illumination of monochromatic light. As shown in **Figure 4**, the valley of the EQE profile from the blend of TQ1:[60]PCBM disappeared in going to the blend of TQ1:[70]PCBM, which is consistent with their corresponding absorption spectra (Figure 1). The device from TQ1:[70]PCBM shows a considerably high photo-conversion efficiency in the range of 370–650 nm with EQE values of 50–60%. The J_{sc} calculated from integration of the EQE of the device with an AM 1.5G reference spectrum is 10.9 mA cm^{-2}, which is rather close to the J_{sc} (10.5 mA cm^{-2}) obtained from the *J*–*V* measurement with a difference smaller than 4%. This result shows that TQ1 is among the best conjugated polymers for BHJ polymer solar cells reported to date.

For optimization of the devices from the blend of TQ1:[70]PCBM, over 500 devices were fabricated with different ratios (1:1, 1:2, 1:3 and 1:4) and film thicknesses from 50 nm to 330 nm (see supporting information). The performance of the devices is quite scattered, probably due to a high sensitivity to small variations in the morphology of the active layers. Over 30 optimal devices with thickness of 70–95 nm showed MPP between 5.2 mW cm^{-2} and 6.2 mW cm^{-2}. Certification experiments

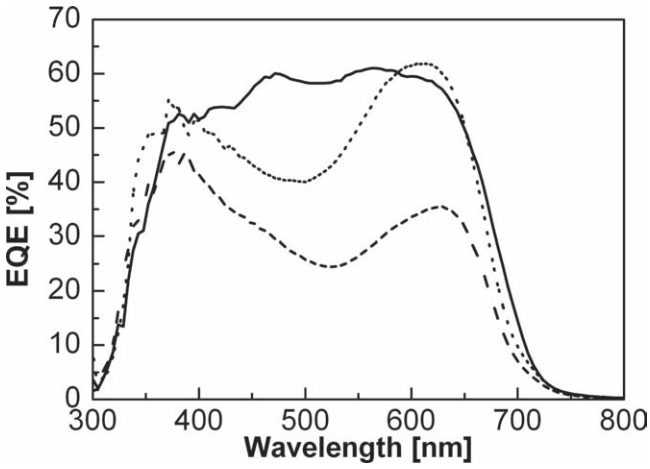

Figure 4. The EQE profiles of the devices from TQ1:[60]PCBM = 1:3 in chloroform solution (dashed line), TQ1:[60]PCBM = 1:3 in ODCB solution (dotted line) and TQ1:[70]PCBM = 1:3 in ODCB solution (solid line).

will be performed in the near future. Moreover, the reproducibility of high efficiency solar cells is a miserable problem due to the differences in purity and molecular weights for different batches of polymers.[31] It's worth noting that high MPP over 6 mW cm^{-2} can be repeated by different batches of TQ1.

In conclusion, an easily synthesized D-A type polymer TQ1 was investigated for application in polymer solar cells. The polymer shows promising photophysical properties with a broad absorption spectrum and an optical bandgap of 1.70 eV, meanwhile the HOMO and LUMO levels are located in suitable position matching with those of PCBMs and keeping a high V_{oc} about 0.9 V. Based on the excellent photophysical and electrochemical properties, a MPP up to 6 mW cm^{-2} (corresponding to PCE of 6%) was achieved by simply processed devices, which demonstrates TQ1 to be a particularly promising candidate for high efficiency polymer solar cells. In addition, the simple structure of TQ1 offers a bright future for commercialization as an alternative to the widely investigated P3HT.

Experimental Section

Characterization: ^{1}H NMR and ^{13}C NMR spectra were acquired from a Varian Inova 500 MHz NMR spectrometer. Tetramethylsilane was used as an internal reference with deuterated chloroform as solvent. Size exclusion chromatography (SEC) was performed on Waters Alliance GPCV2000 with a refractive index detector columns: Waters Styvagel HT GE × 1, Waters Styvagel HMW GE × 2. The eluent was 1,2,4-trichlorobenzene. The working temperature was 135 °C, and the resolution time was 2 h. The concentration of the samples was 0.5 mg mL^{-1}, which was filtered (filter: 0.45 μm) prior the analysis. The molecular weights were calculated according relative calibration with polystyrene standards. UV-vis absorption spectra were measured with a Perkin Elmer Lambda 900 UV-Vis-NIR absorption spectrometer. Square-wave voltammetry (SWV) measurements were carried out on a CH-Instruments 650A Electrochemical Workstation. A three-electrode setup was used with platinum wires both as working electrode and counter electrode, and Ag/Ag^+ used as reference electrode calibrated with Fc/Fc^+. A 0.1 M solution of tetrabutylammonium hexafluorophosphate (Bu_4NPF_6) in anhydrous acetonitrile was used as supporting electrolyte. The polymers were deposited onto the working electrode from chloroform solution. In order to remove oxygen from the electrolyte, the system was bubbled with nitrogen prior to each experiment. The nitrogen inlet was then moved to above the liquid surface and left there during the scans. HOMO and LUMO levels were estimated from peak potentials of the third scan by setting the oxidative peak potential of Fc/Fc^+ *vs.* the normal hydrogen electrode (NHE) to 0.63 V,[32] and the NHE *vs.* the vacuum level to 4.5 V.[33]

Synthetic Procedures: All reagents were purchased from commercial sources and used without further purification.

5,8-dibromo-2,3-bis(3-(octyloxy)phenyl)quinoxaline (**1**): To a suspension of zinc (5 g, 77 mmol) and 4,7-dibromobenzo[c][1,2,5]thiadiazole (4.41 g, 15 mmol) in acetic acid (100 mL), a few drops of water was added. The mixture was stirred at 60 °C for 6 h. After that, the solid residue was removed by filtration. And then 1,2-bis(3-(octyloxy)phenyl)ethane-1,2-dione (6 g, 12.9 mmol) was added to the filtrate. The resulting solution was stirred at 60 °C overnight. The mixture was transferred to a separatory funnel, extracted with diethyl ether and then washed with water. The ether phase was dried over $MgSO_4$. The crude product was purified by silica-gel column chromatography with a mixture of hexane:dichloromethane = 1:1 as eluent to obtain the pure product as a yellow solid (7.91 g, 88%). ^{1}H NMR (500 MHz, $CDCl_3$, δ): 7.92 (s, 2H), 7.24 (m, 4H), 7.19 (d, J = 6.6 Hz, 2H), 6.93 (d, J = 7.8 Hz, 2H), 3.86 (t, 4H; OCH_2), 1.73 (m, 4H; CH_2), 1.30–1.43 (m, 20H; CH_2), 0.89 (t, 6H; CH_3); ^{13}C NMR (125 MHz, $CDCl_3$, δ): 159.0, 154.0, 139.3, 139.1, 133.1, 129.3, 123.7, 122.5, 116.5, 115.7, 68.1, 31.8, 29.3, 29.2, 29.1, 26.0, 22.7, 14.1.

Poly[2,3-bis-(3-octyloxyphenyl)quinoxaline-5,8-diyl-alt-thiophene-2,5-diyl]: In a 25 mL dry flask, compound **1** (349 mg, 0.5 mmol), **2** (205 mg, 0.5 mmol), tris(dibenzylideneacetone)dipalladium(0) ($Pd_2(dba)_3$) (6 mg) and tri(*o*-tolyl)phosphine ($P(o\text{-}Tol)_3$) (10 mg) were dissolved in degassed toluene (6 mL). The mixture was vigorously stirred at 100 °C for 24 h under nitrogen. After cooling down, the solution was poured into acetone. The polymer was collected by filtration through 0.45 μm Teflon filter. And then the polymer was dissolved in 100 mL of ODCB and mixed with a solution of sodium diethyldithiocarbamate trihydrate (5 g) in distilled water (100 mL). The mixture was stirred at 80 °C overnight under nitrogen. The organic phase was separated and washed three times with water. Then it was poured into 400 mL of acetone. The precipitate was collected by thimble and Soxhlet-extracted with ether and chloroform in order. The chloroform fraction was precipitated in acetone. Finally, the polymer was collected by filtration through 0.45 μm Teflon filter and dried under vacuum at 40 °C overnight (237 mg, 76.6%). ^{1}H NMR (500 MHz, $CDCl_3$, δ): 7.83 (2H), 7.35 (2H), 7.21–7.10 (6H), 6.84 (2H), 3.70 (4H; OCH_2), 1.54 (4H; CH_2), 1.17 (20H; CH_2), 0.80 (6H; CH_3).

Device Fabrication and characterization: The structure of the solar cell is Glass/ITO/PEDOT:PSS/Active Layer/LiF/Al. As a buffer layer, the conductive polymer PEDOT:PSS (Baytron P VP Al 4083) was spin-coated onto ITO-coated glass substrates, followed by annealing at 120 °C for 10 minutes to remove water. The thickness of the PEDOT:PSS layer was about 45 nm, as determined by a Dektak 6M surface profilometer. The active layer consisting of TQ1 and [70]PCBM (or [60]PCBM) was spin-coated from ODCB solution (or chloroform) onto the PEDOT:PSS layer. The active layers were spin-coated in a glove box and directly transferred to a vapor deposition system mounted inside of the glove box. LiF (0.6 nm) and Al (80 nm) were used as top electrodes and were deposited via a mask in vacuum onto the active layer. The accurate area of every device defined by the overlap of the ITO and metal electrode was measured carefully by microscope image (4–6 mm^2). EQEs were calculated from the photocurrents at short-circuits conditions. The currents were recorded by a Keithley 485 picoammeter under illumination of monochromatic light (MS257) through the ITO side of the devices. MPP was calculated from *J–V* characteristics recorded by a Keithley 2400 Source meter under illumination of an AM1.5G solar simulator with an intensity of 100 mW cm^{-2} (Model SS-50A, Photo Emission Tech., Inc.). The light intensity was determined by a standard silicon photodiode. Device characterization was conducted in ambient environment. Here we report the MPP, as obtained from the experimental determinations of PCE with the solar

simulator, which is equivalent to the PCE as previously reported from this lab. Due to the spectral mismatch between the plastic solar cells and the reference silicon photodiode, some error is introduced in this measurement. Considering this error, we report MPP rather than PCE.

Supporting Information

Supporting Information is available from the Wiley Online Library or from the author.

Acknowledgements

We thank the Swedish Energy Agency for financial support through projects Polarge. The authors thank Dr. Timothy Steckler for helpful discussions.

Received: June 18, 2010
Revised: July 22, 2010
Published online: September 8, 2010

[1] G. Dennler, M. C. Scharber, C. J. Brabec, *Adv. Mater.* **2009**, *21*, 1323.
[2] M. Helgesen, R. Sondergaard, F. C. Krebs, *J. Mater. Chem.* **2010**, *20*, 36.
[3] F. C. Krebs, *Sol. Energy Mater. Sol. Cells* **2009**, *93*, 394.
[4] B. C. Thompson, J. M. J. Fréchet, *Angew. Chem. Int. Ed.* **2008**, *47*, 58.
[5] G. Yu, J. Gao, J. C. Hummelen, F. Wudl, A. J. Heeger, *Science* **1995**, *270*, 1789.
[6] W. L. Ma, C. Y. Yang, X. Gong, K. Lee, A. J. Heeger, *Adv. Funct. Mater.* **2005**, *15*, 1617.
[7] G. Li, V. Shrotriya, J. S. Huang, Y. Yao, T. Moriarty, K. Emery, Y. Yang, *Nat. Mater.* **2005**, *4*, 864.
[8] H. Y. Chen, J. H. Hou, S. Q. Zhang, Y. Y. Liang, G. W. Yang, Y. Yang, L. P. Yu, Y. Wu, G. Li, *Nat. Photonics* **2009**, *3*, 649.
[9] S. H. Park, A. Roy, S. Beaupré, S. Cho, N. Coates, J. S. Moon, D. Moses, M. Leclerc, K. Lee, A. J. Heeger, *Nat. Photonics* **2009**, *3*, 297.
[10] M. Svensson, F. L. Zhang, S. C. Veenstra, W. J. H. Verhees, J. C. Hummelen, J. M. Kroon, O. Inganäs, M. R. Andersson, *Adv. Mater.* **2003**, *15*, 988.
[11] L. H. Slooff, S. C. Veenstra, J. M. Kroon, D. J. D. Moet, J. Sweelssen, M. M. Koetse, *Appl. Phys. Lett.* **2007**, *90*, 143506.
[12] E. G. Wang, M. Wang, L. Wang, C. H. Duan, J. Zhang, W. Z. Cai, C. He, H. B. Wu, Y. Cao, *Macromolecules* **2009**, *42*, 4410.
[13] M. H. Chen, J. Hou, Z. Hong, G. Yang, S. Sista, L. M. Chen, Y. Yang, *Adv. Mater.* **2009**, *21*, 4238.
[14] F. L. Zhang, J. Bijleveld, E. Perzon, K. Tvingstedt, S. Barrau, O. Inganäs, M. R. Andersson, *J. Mater. Chem.* **2008**, *18*, 5468.
[15] E. G. Wang, L. Wang, L. F. Lan, C. Luo, W. L. Zhuang, J. B. Peng, Y. Cao, *Appl. Phys. Lett.* **2008**, *92*, 033307.
[16] J. Hou, H.-Y. Chen, S. Zhang, G. Li, Y. Yang, *J. Am. Chem. Soc.* **2008**, *130*, 16144.
[17] Y. Y. Liang, D. Q. Feng, Y. Wu, S. T. Tsai, G. Li, C. Ray, L. P. Yu, *J. Am. Chem. Soc.* **2009**, *131*, 7792.
[18] R. P. Qin, W. W. Li, C. H. Li, C. Du, C. Veit, H. F. Schleiermacher, M. Andersson, Z. S. Bo, Z. P. Liu, O. Inganäs, U. Wuerfel, F. L. Zhang, *J. Am. Chem. Soc.* **2009**, *131*, 14612.
[19] T. Yamamoto, B. L. Lee, H. Kokubo, H. Kishida, K. Hirota, T. Wakabayashi, H. Okamoto, *Macromol. Rapid. Commun.* **2003**, *24*, 440.
[20] M. H. Lai, C. C. Chueh, W. C. Chen, J. L. Wu, F. C. Chen, *J. Polym. Sci., Part A: Polym. Chem.* **2009**, *47*, 973.
[21] L. Huo, Z. A. Tan, X. Wang, Y. Zhou, M. Han, Y. Li, *J. Polym. Sci., Part A: Polym. Chem.* **2008**, *46*, 4038.
[22] A. Gadisa, W. Mammo, L. M. Andersson, S. Admassie, F. Zhang, M. R. Andersson, O. Inganäs, *Adv. Funct. Mater.* **2007**, *17*, 3836.
[23] Z. Zhu, D. Waller, R. Gaudiana, M. Morana, D. Mühlbacher, M. Scharber, C. Brabec, *Macromolecules* **2007**, *40*, 1981.
[24] J. Peet, J. Y. Kim, N. E. Coates, W. L. Ma, D. Moses, A. J. Heeger, G. C. Bazan, *Nat. Mater.* **2007**, *6*, 497.
[25] M. M. Wienk, M. Turbiez, J. Gilot, R. A. J. Janssen, *Adv. Mater.* **2008**, *20*, 2556.
[26] R. C. Coffin, J. Peet, J. Rogers, G. C. Bazan, *Nat. Chem.* **2009**, *1*, 657.
[27] S. Hellström, F. L. Zhang, O. Inganäs, M. R. Andersson, *Dalton Trans.* **2009**, 10032.
[28] M. C. Scharber, D. Wühlbacher, M. Koppe, P. Denk, C. Waldauf, A. J. Heeger, C. J. Brabec, *Adv. Mater.* **2006**, *18*, 789.
[29] M. M. Wienk, J. M. Kroon, W. J. H. Verhees, J. Knol, J. C. Hummelen, P. A. van Hal, R. A. J. Janssen, *Angew. Chem. Int. Ed.* **2003**, *42*, 3371.
[30] X. J. Wang, E. Perzon, F. Oswald, F. Langa, S. Admassie, M. R. Andersson, O. Inganäs, *Adv. Funct. Mater.* **2005**, *15*, 1665.
[31] J. K. Lee, W. L. Ma, C. J. Brabec, J. Yuen, J. S. Moon, J. Y. Kim, K. Lee, G. C. Bazan, A. J. Heeger, *J. Am. Chem. Soc.* **2008**, *130*, 3619.
[32] V. V. Pavlishchuk, A. W. Addison, *Inorg. Chim. Acta.* **2000**, *298*, 97.
[33] A. J. Bard, L. R. Faulkner, *Electrochemical methods: fundamentals and applications*, Wiley, New York **2001**.